Spatial scale and cellular substrate of contrast adaptation by retinal ganglion cells

Solange P. Brown[1] and Richard H. Masland[1,2]

[1] *Program in Neuroscience, Goldenson 228, Harvard Medical School, Boston, Massachusetts 02115, USA*

[2] *Howard Hughes Medical Institute, Wellman 429, Massachusetts General Hospital, Boston, Massachusetts 02114, USA*

Correspondence should be addressed to R.H.M. (masland@helix.mgh.harvard.edu)

Human visual perception and many visual system neurons adapt to the luminance and contrast of the stimulus. Here we describe a form of contrast adaptation that occurs in the retina. This adaptation had a local scale smaller than the dendritic or receptive fields of single ganglion cells and was insensitive to pharmacological manipulation of amacrine cell function. These results implicate the bipolar cell pathway as a site of contrast adaptation. The time required for contrast adaptation varied with stimulus size, ranging from approximately 100 ms for the smallest stimuli, to seconds for stimuli the size of the receptive field. The differing scales and time courses of these effects suggest that multiple types of contrast adaptation are used in viewing natural scenes.

Sensory systems must maintain sensitivity to small gradations in their inputs despite huge ranges in the absolute strength of those inputs, a combined requirement that far outstrips the limited capacity of neurons for transmitting information. A strategy for overcoming this limitation is adaptation, during which systems shift their operating range to match the prevailing stimulus strength. The retina contains a number of adaptive mechanisms, working over different time courses and spatial scales, that center a ganglion cell's limited response range around a scene's mean luminance. The ganglion cell then encodes excursions from this mean (for review, see ref. 1).

The retina also regulates its sensitivity to contrast. Spatial contrast is the range of luminances of objects in a visual image; temporal contrast is the range of luminances, for the same point in a visual image, at different times. Classic studies established that changes in stimulus contrast averaged over several millimeters of retina rapidly (~100 ms) cause a ganglion cell's sensitivity to decrease in the face of a high-contrast stimulus and increase in response to low-contrast[2–7]. More recently, a second, much slower adjustment of the ganglion cell's response, with a time course of tens of seconds, was identified[8], in which, again, a ganglion cell's response is decreased in the presence of high-contrast stimuli and vice versa. However, in this case, the change evolves more slowly than the previously described contrast gain control. Because of this difference and other dissimilarities[9], the two processes have been provisionally distinguished as 'contrast gain control' and 'contrast adaptation,' respectively.

Our initial goal was to identify the cellular basis of the slow form of retinal contrast adaptation, and our first question addressed the spatial distribution of contrast adaptation. We individually stimulated subregions of the receptive fields of retinal ganglion cells and asked whether separate regions within a ganglion cell's receptive field adapt individually. Can the center and surround each adapt to contrast? Can two small regions within the receptive field center adapt independently? The results of these experiments implicated a small-field element in the detection of contrast, the major candidates being narrow-field amacrine cells or bipolar cells. In a second set of experiments, we tested whether blocking the receptors of the major neurotransmitters of most amacrine cells, glycine and γ-aminobutyric acid (GABA), had an effect on contrast adaptation.

Results

The response to step increases and decreases in contrast from one cell is shown in Fig. 1. The checkerboard stimulus consisted of 25 squares whose luminances were independently modulated; the contrast of the entire stimulus was abruptly changed every 45 s. Following abrupt increases in contrast, the cell fired strongly at first and progressively reduced its firing rate during each 45-s epoch. Following a step decrease in contrast, the cell stopped firing action potentials completely and then gradually increased its firing rate during each low-contrast epoch.

The responses of the cell to a pulse of light (the impulse responses) were derived from the spike-triggered stimulus average for different delays following a step increase in contrast (**Fig. 1d**). The amplitude of the impulse response decreased several fold during the high-contrast epochs. The same visual contrast thus elicited progressively fewer action potentials as the cell adapted to the high-contrast stimulus, indicating that a change in the cell's sensitivity evolved over many seconds. At these time scales, we did not see any corresponding changes in the temporal features of the impulse response[8,9].

Of the 47 cells examined, 41 (87%) showed similar changes in firing rate in response to step increases and decreases in contrast. These cells included ON and OFF alpha cells, ON-OFF direction-selective cells and ON direction-selective cells, identified using physiological and morphological criteria (see Methods). Additional types of ON and OFF ganglion cells also adapted to contrast, including the ON-sustained cell in Fig. 1. There was some variability in the details of the responses, including the amount

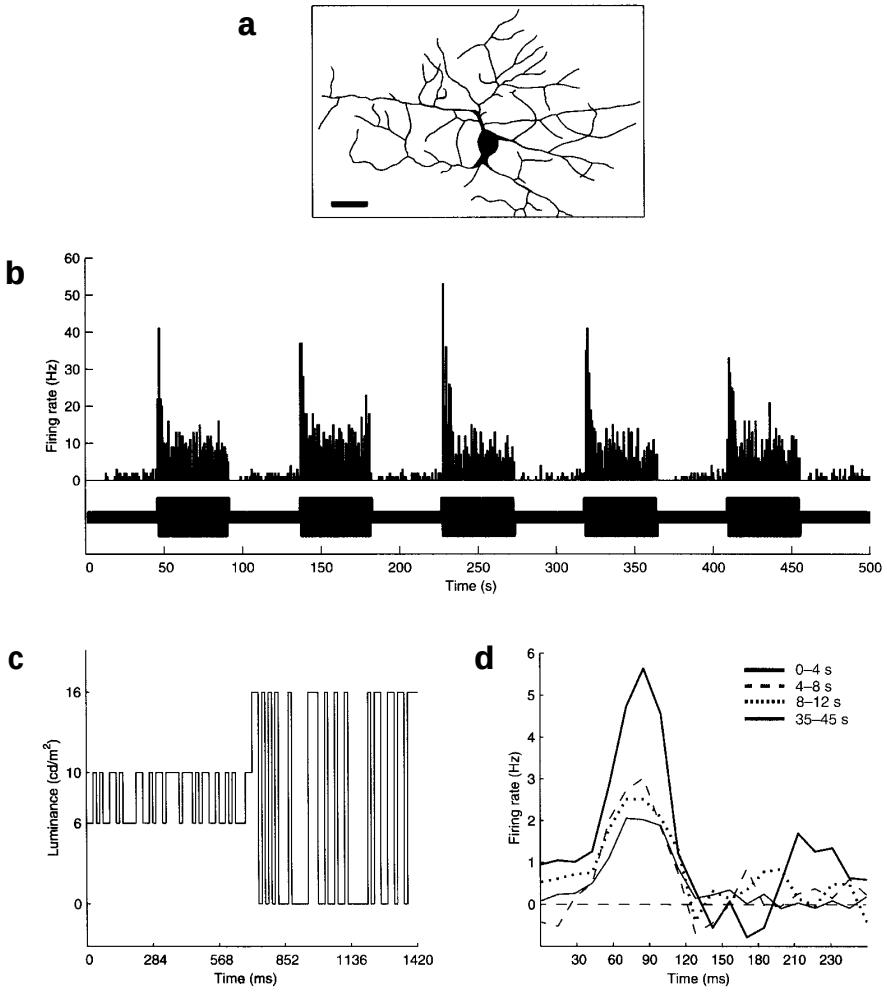

Fig. 1. Ganglion cell responses to abrupt changes in stimulus contrast. (**a**) The morphology of the cell whose responses are shown in (**b**) and (**d**). The cell soma appears large because of flare from the large concentration of Lucifer Yellow in the cell body. Scale bar, 50 μm. (**b**) The responses of this ON-sustained cell to five individual step increases in contrast and six step decreases in contrast (bin-width, 1 s) of a 5 × 5 checkerboard pattern (520 μm × 520 μm) centered over the receptive field center. The trace below the histogram of spike rate indicates the contrast (25% or 100%) of the checkerboard pattern, which changed abruptly every 45 s. The spatiotemporal stimulus was updated every 14.2 ms (every video frame) and was different for each contrast epoch. The temporal structure of the stimulus is not visible at this time scale. (**c**) The intensity of one pixel of the visual stimulus in (**b**) shown at an expanded time scale. (**d**) The impulse response of the receptive field center for different periods following the transition to high-contrast. The change in the impulse response reflects a gradual decrease in sensitivity of the cell over time. The impulse response was calculated using 14.2 ms time bins and 24 high-contrast/low-contrast stimulus pairs.

and time course of the adaptation (as has been noted for lateral geniculate nucleus and visual cortical neurons[10–12]). Despite this variability, many types of rabbit retinal ganglion cells clearly share the fundamental property of contrast adaption. No systematic differences were identified among the different ganglion cell types.

For many cells, a single exponential did not adequately describe the changes in firing rate following abrupt changes in contrast, similarly to contrast adaptation of cat cortical neurons[10,11,13]. We therefore used other indices[10] to summarize features of the adaptation (see Methods). For 24 cells tested with the same contrast pairs, the adaptation index (AI) was always greater than 1 for the high-contrast epochs (AI ± s.d., 2.4 ± 1.4; time bin, 1 s). In other words, the firing rates of all cells tested decreased during the high-contrast epochs. The mean decay index was 3.4 s (range, 1–10 s; time bin, 1 s). Following decrease in contrast, behavior of cells was more varied. All 24 cells abruptly decreased their firing rates, but 10 of the 24 cells' recoveries did not reach our criterion for adaptation (see Methods); their firing rates were still very low at the end of the 45-s epochs. (Recovery to downward contrast steps was also observed for only about half of rabbit cells in a previous study[8].) However, the remaining 14 cells' firing rates almost tripled on average over the course of the low-contrast epochs (45 s; AI = 0.38 ± 0.25; time bin, 1 s). For the low-contrast epochs, the mean recovery index was 7.6 s (range, 2–19 s; time bin, 1 s).

Contrast adaptation of the receptive field surround

We separately stimulated the center and surround of individual ganglion cells, asking whether or not these two regions of the receptive field could be independently adapted. If the spatial extent of the neural element sampling the contrast of the visual scene is larger than the receptive field of ganglion cells, this element—such as a wide-field amacrine cell[14–16]—would be expected to average the contrast over a large area (> 500 μm) and pass this signal to both the center and surround circuitry of the ganglion cell.

A ganglion cell's response to step changes in contrast with the stimulus confined to the receptive field center is shown in Fig. 2b. Following step increases in contrast, the cell abruptly increased its firing rate; its firing rate then gradually decreased during the high-contrast epochs. (A similar response was seen for a stimulus that covered both the center and the surround; data not shown.) Following abrupt decreases in contrast, the cell sharply decreased its firing rate, which then gradually increased during the remainder of the low-contrast periods.

When changes in contrast were confined to the surround, the cell's firing rate showed little change from its average activity during mean luminance (**Fig. 2c**). To reveal the effect of stimulating the surround, we stimulated the center at a constant contrast, while abruptly increasing and decreasing the contrast of the stimulus in the surround; the center stimulus produced a steady firing rate,

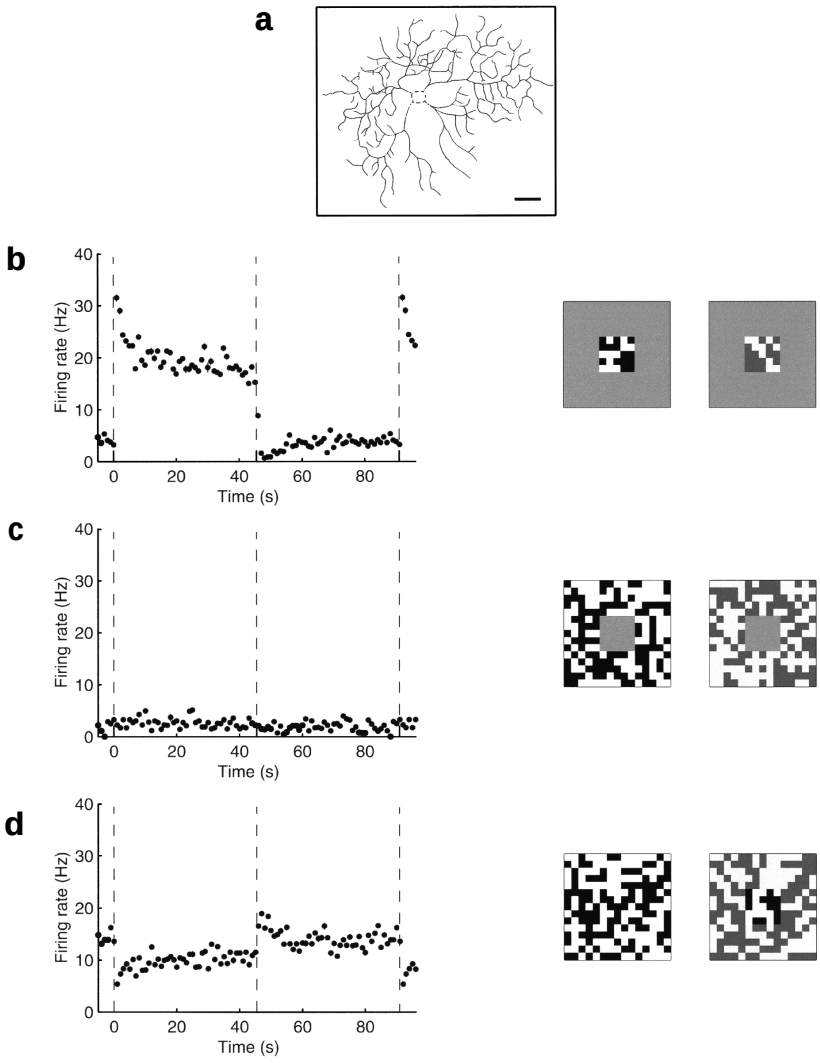

Fig. 2. The response of a ganglion cell to abrupt changes in contrast in the receptive field center versus receptive field surround. (**a**) The morphology of the cell whose responses are described in (**b–d**). Scale bar, 50 μm. (**b–d**) Left, the averaged response of the cell to 10 stimulus pairs; right, schematic of the stimulus pair used. Here, and in all subsequent figures, segments of the periodic data are replotted to the left and right of the outside dashed lines for clarity. (**b**) The average response of the ganglion cell to abrupt changes in contrast confined to the receptive field center (binwidth, 1 s). (**c**) The response of the cell to abrupt changes in contrast confined to the receptive field surround (binwidth, 1 s). (**d**) The response of the cell to abrupt changes in contrast in the surround while the receptive field center was continuously stimulated with a high-contrast stimulus (binwidth, 1 s). The time courses are comparable for the center and surround, even though the absolute firing rates are very different.

which could be modulated by the surround stimulus. Under these conditions, contrast changes in the surround (**Fig. 2d**) produced effects opposite to those for the receptive field center (**Fig. 2b**). Following abrupt increases in contrast of the surround stimulus, the cell decreased its firing rate, which then gradually recovered. Abrupt decreases in surround contrast caused the cell's firing to increase. This firing rate decreased during the low-contrast epochs.

We compared the effects of abrupt changes in contrast in the center versus the surround for the seven ganglion cells tested, including both ON and OFF cells (**Fig. 3**). For all cells tested, increased contrast in the center of the receptive field center caused abrupt increases in firing rate that gradually decreased during the high-contrast epoch, whereas step decreases in contrast elicited abrupt decreases in firing rates, which slowly recovered in three cells. Changes in the contrast of stimuli confined to the receptive field surround produced effects opposite in polarity to changes caused by center stimuli. Following abrupt increases in the contrast of the surround stimulus, five of seven cells abruptly decreased their firing rate; this firing rate gradually increased for four cells during the high-contrast epochs (**Fig. 3**). Six of the seven cells tested abruptly increased their firing rates following step decreases in the contrast of the surround stimulus. The firing rate of four cells then gradually decayed during the low-contrast epochs (**Fig. 3**). The mean recovery rate was 2.5 s (time bin, 1 s), whereas the mean decay rate was 4.0 s (time bin, 1 s). In summary, the surround of rabbit ganglion cells adapted to contrast independently of the center mechanism, with a time course similar to the one seen for the receptive field center. Therefore, the elements mediating contrast adaptation must have a spatial extent no larger than the receptive field center of the ganglion cell.

Response to local changes of contrast

In an additional set of experiments, we asked whether subregions of the receptive field center of a ganglion cell would separately adapt to contrast. During each epoch in these experiments, 4 squares, each 104 μm across, were modulated against a background of mean luminance. The adapting stimulus alternated between two locations within the receptive field center.

If the ganglion cell (or a neuron with a similarly sized receptive field) spatially averaged the contrast of the visual scene impinging on its receptive field, then there should be little or no change in the ganglion cell's firing when the location of the small, adapting stimulus is alternated back and forth in its receptive field center. Alternatively, if a narrow-field element with a receptive field smaller than a ganglion cell—such as a narrow-field amacrine or bipolar cell—underlies contrast adaptation, the array of those narrow-field cells would resolve these small, local changes in contrast. Figure 4 shows the results from two cells. The firing rate of each cell increased abruptly when the contrast was increased at either location of the small stimuli (**Fig. 4**). The firing rate then decayed to a baseline level.

For the seven cells, both ON and OFF, tested in a similar fashion, the cells' firing rate adapted when the contrast at the two locations was alternated (**Fig. 5**). The maximum spike rate immediately following the contrast change was on average 2.4 ± 0.7 times greater than the baseline firing rate, ranging from 8 to 59 Hz (time bin, 100 ms). However, the time course of these effects was much faster

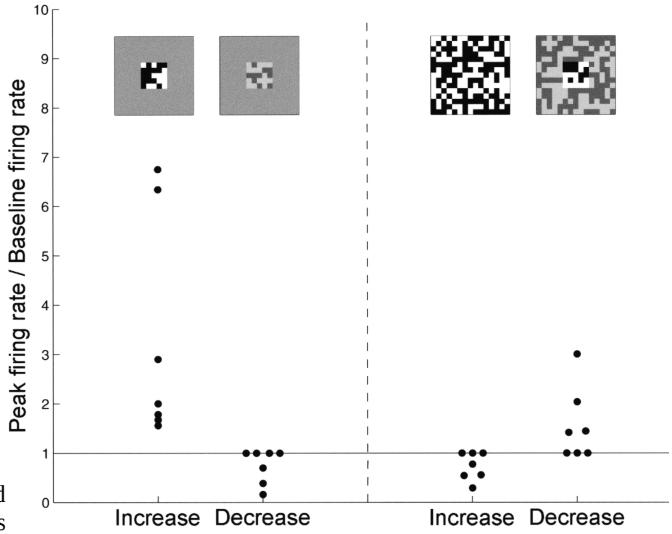

Fig. 3. The responses of ganglion cells, including ON and OFF cells, to contrast changes for stimuli confined to the receptive field center compared to stimuli confined to the receptive field surround. The adaptation index for the stimulus pairs shown in Fig. 2b and d is plotted (binwidth, 500 ms). If there were no significant change in the firing rate of the cell over the contrast epochs, the adaptation index would be one and would fall on the solid horizontal line. Decays in firing rate result in an adaptation index greater than one, whereas increases in firing rate result in an adaptation index less than one. When more than one cell had the same adaptation index, the data points were offset horizontally for clarity. The polarity of the contrast adaptation reversed when the contrast changes occured in the receptive field surround rather than the receptive field center. For 4 cells, the responses over 24 stimulus pairs was averaged, while 19, 14 and 10 stimulus pairs were used for the 3 remaining cells.

than the contrast adaptation observed for larger checkerboard stimuli; the decay indices ranged from 0 to 800 ms for the 7 cells tested (time bin, 100 ms).

Even though the firing rates elicited by these small stimuli were lower than the rates achieved when stimulating the entire receptive field center (compare the *y*-axes in **Fig. 4a**), these stimuli still caused each ganglion cell to adapt its firing rate. These responses were not simply the result of different regions of the receptive field being differentially sensitive. If the adapting stimulus alternated between a region of high and a region of low sensitivity, the ganglion cell would respond as though it were seeing a high-contrast epoch (such as a patch over more sensitive region) followed by a low-contrast epoch (such as a patch over less sensitive region). Thus, the ganglion alone could not simply be averaging the contrast of a visual scene impinging on its receptive field. Instead, cells with small receptive fields presynaptic to the ganglion cell must at least partly underlie these local effects.

Adaptation following blockade of glycine receptors

Two possible candidates for involvement in ganglion cell adaptation are the narrow-field amacrine cells and the bipolar cells. If an amacrine cell circuit underlies the phenomenon of contrast adaptation, its function should be revealed by perturbing the major neurotransmitter systems used by amacrine cells, GABA and glycine[14,17–19]. Bipolar cells, on the other hand, are glutamatergic[20].

Strychnine, an antagonist of glycine receptors, produced little change in contrast adaptation for the three ON and one OFF cells tested. In no case was the ganglion cell's adaptation to contrast eliminated (**Fig. 6**). Under all three conditions (control, drug and recovery), the amplitude of the impulse response gradually decreased during the high-contrast epoch (data not shown). Strychnine did not significantly change the decay (mean, 1.75 s; range, 1–3, versus mean, 2.5 s; range, 1–5; time bin, 1 s) and recovery indices (mean, 8.6 s; range, 6–10, versus mean, 7.3 s; range, 3–11; time bin, 1 s) for the cells. Although the firing rate in the presence of glycinergic receptor blockade was markedly elevated as compared to the control and recovery conditions, the overall character of the response was very similar. These results suggested that a glycinergic amacrine cell is not fundamentally important in the slow-contrast adaptation of these retinal ganglion cells.

These results also confirmed that the effects seen were not solely caused by fatigue *per se* of the spike generating mechanism of the ganglion cell. The firing rates of the cells were increased in the presence of strychnine (**Fig. 6c**), yet their adaptation indices were similar in the presence and absence of glycinergic receptor blockade (**Fig. 6d**).

Adaptation following blockade of GABA receptors

Picrotoxin blocks $GABA_A$ receptors and most mammalian $GABA_C$ receptors[21]. Although the response of the cell to step increases and decreases in contrast was greatly amplified in the presence of picrotoxin, the basic features of contrast adaptation were still present (**Fig. 7a**). Similar effects were seen in all six cells tested, both ON and OFF (**Fig. 7c** and **d**). In no case did picrotoxin attenuate the cell's ability to adapt to abrupt contrast changes. The decay (mean, 5.8 s; range, 2–10 versus mean, 6.7 s, range, 4-9; time bin, 1 s) and the recovery indices (mean, 13.3 s; range, 5–19, versus mean, 11.7 s; range, 7–17; time bin, 1 s) were not markedly different between the two conditions. (A preliminary experiment with the $GABA_B$ receptor agonist baclofen suggested that $GABA_B$ receptors do not contribute significantly to contrast adaptation; data not shown.) Like the experiments using strychnine, these experiments suggested that adaptation can be dissociated from the firing rates of the cell. In extreme cases, the firing rate was increased 10 fold and yet, the ratios of the adaptation indices under the two conditions were approximately one (**Fig. 7c** and **d**).

Discussion

Our evidence suggests that the site of contrast adaptation in these experiments lies along a narrow-field pathway of the retina. Adaptation did not spread laterally; the center and surround of a receptive field could be adapted separately, with opposite effects on the overall firing of the ganglion cell. Furthermore, subregions of the receptive field center could be separately adapted. The independently adaptable regions were much smaller than the receptive field center of the ganglion cell.

These results immediately rule out a global mechanism within the ganglion cell. They also rule out a contribution from horizontal cells or the 25% of amacrine cells that have wide-field arborizations[16]. The processes of the retinal ganglion cells at 6–10 mm eccentricity span 200 to 800 μm. Dendrites of individual horizontal cells span approximately 200 μm and are strongly coupled via gap junctions[22]. Those of the 25% of amacrine cells described as wide-field[14–16] range from a minimum of ~500 μm for starburst cells to several millimeters. The average contrast within the spatial extent of these wide-field cells would remain essentially the same under our experimental protocols. It is conceivable that local neuronal subunits within some wide-field amacrines could function independently of the whole cell and mediate the local effects

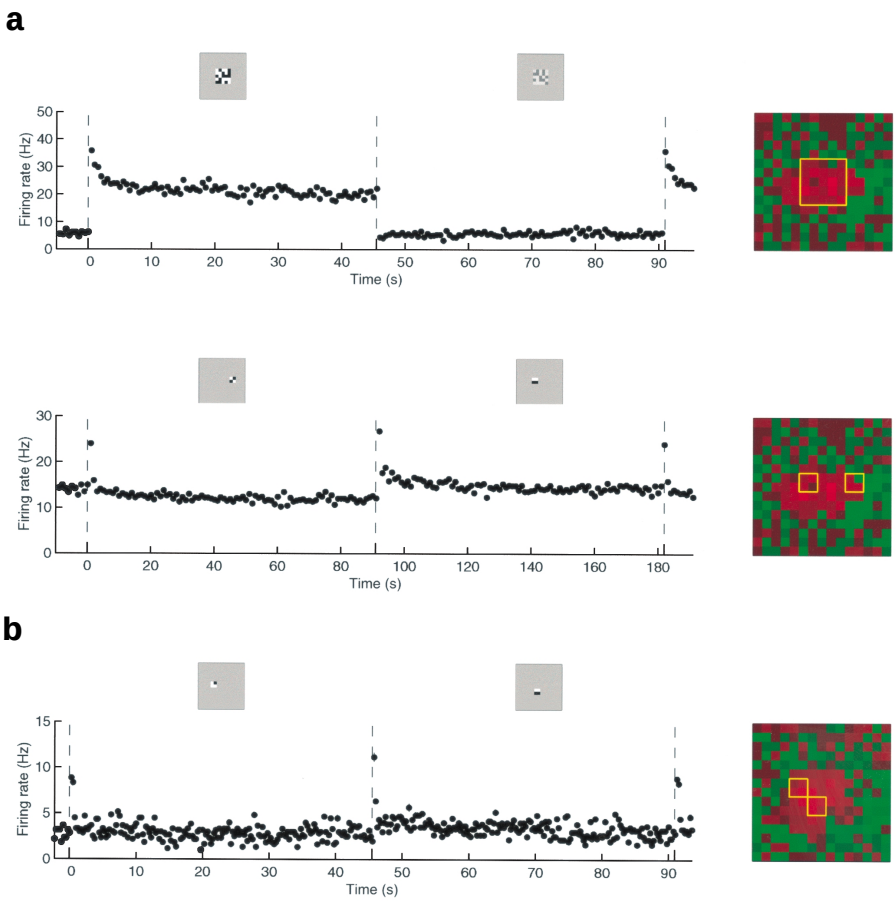

Fig. 4. The response of two OFF ganglion cells to local changes in contrast confined to the receptive field center. The response of the cell is shown in the left panel of each row. The yellow boxes mark the location of the visual stimulus relative to the cell's receptive field in the right panel. The receptive field is the spike-triggered average[42,43] shown at a delay of 42.6 ms before the action potential in each case (see Methods). (**a**) Top, the response of a cell to contrast changes over a large portion of the receptive field center (binwidth, 500 ms). Bottom, the response of that cell stimulated with four squares, each 104 μm on a side, that were independently modulated every 14.2 ms. The contrast for the four squares was 100% while the background was maintained at mean luminance. The location of the four squares alternated between two positions as illustrated on the right. When the location of the small patch of high-contrast was abruptly changed, the firing rate of the cell increased and then gradually returned to a baseline level during the 45-s epochs (binwidth, 500 ms). (**b**) A different cell was stimulated as in (**a**). The location of the four squares alternated between the two positions illustrated on the right. When the location of the small patch of high-contrast was abruptly alternated, the firing rate of the cell sharply increased and then quickly returned to a baseline level during the 45 s epochs (binwidth, 250 ms).

we observed. However, even for starburst cells, the smallest wide-field neurons, patch recordings show that the smallest imaginable local subunit spans 200–300 μm[23,24]. The wider cells have long and sparse dendrites, and all that have been carefully studied make sodium action potentials[25–27]. Both findings make it unlikely that short segments of these processes could act on the 100–200 μm scale required by local contrast adaptation.

In contrast, 5 to 20 of each of the various types of narrow-field cells (bipolar or amacrine) are contained within the diameter of a dendritic arbor of a ganglion cell at these eccentricities[16,28–31]. Treatment of the retina with antagonists to $GABA_A$, $GABA_C$ and glycine receptors did not eliminate contrast adaptation. Although a few amacrine cells colocalize catecholamines or peptide neurotransmitters together with GABA, all of these are wide-field cells[14], whose participation is unlikely considering our first set of experiments. The site of adaptation thus seems to reside somewhere along the bipolar cell pathway. Indeed, patch recordings using slices of salamander retina confirm the existence of temporal contrast adap-

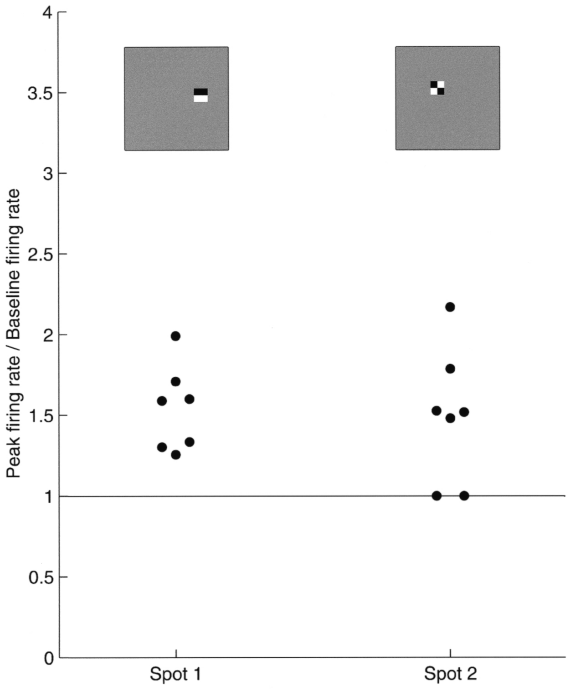

Fig. 5. The responses of ganglion cells, including both ON and OFF types, to contrast changes for stimuli within the receptive field center. The adaptation index is plotted (binwidth, 1 s) for pairs of stimuli like those shown in Fig. 4. Increases in firing rate followed by a decay result in an adaptation index greater than one. For the 7 cells, the adaptation index was greater than one for the two local stimuli tested for all but 2 of the 14 locations, where the adaptation index was not significant (see Methods).

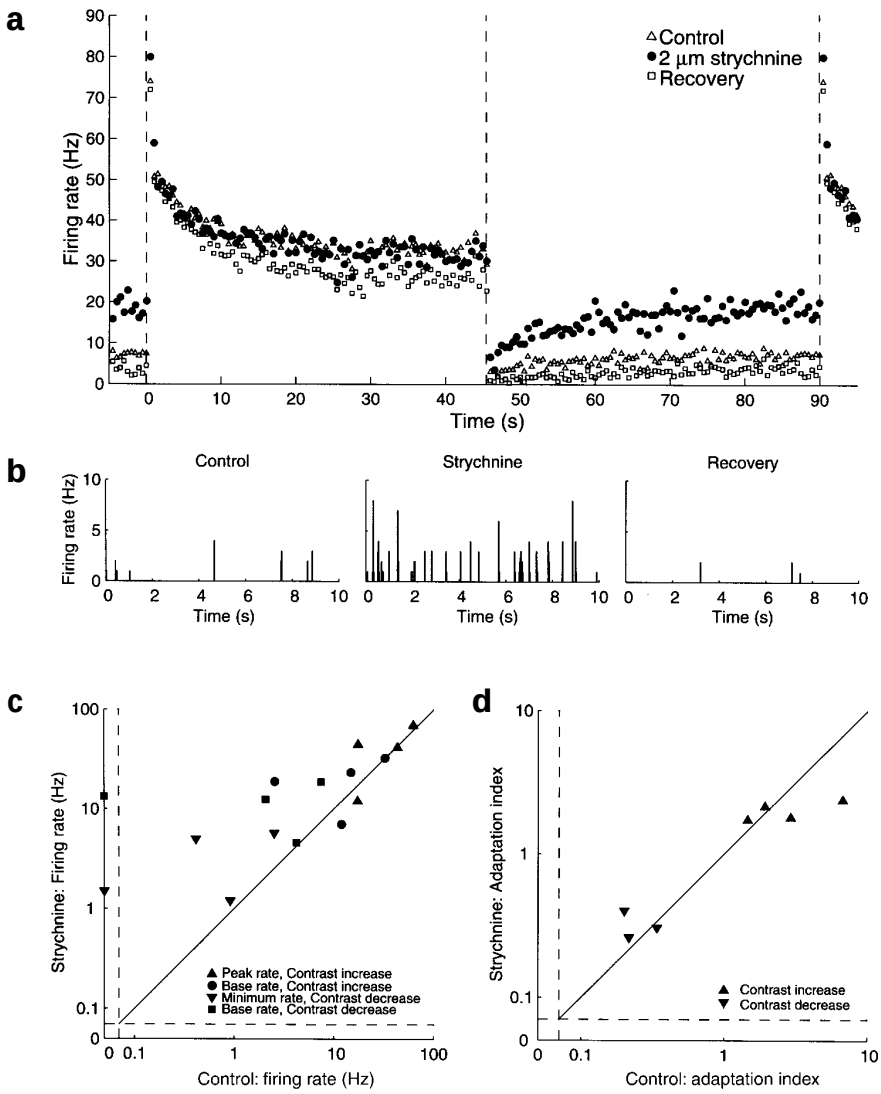

Fig. 6. Contrast adaptation in the presence of a glycine receptor antagonist, strychnine. (**a**) The response to step changes in contrast for one ON cell under control, 2 μM strychnine, and recovery conditions. Qualitatively, the cell responded very similarly to abrupt increases and decreases of contrast under all three conditions. In (**b**), the cell's response to mean luminance is shown for the three conditions. The spike histograms (binwidth, 15 ms) illustrate the dramatic increase in the cell's activity in the presence of strychnine (middle) as compared to the control and recovery conditions (left and right). This positive control indicated that the antagonist clearly affected the behavior of this ganglion cell. (**c**, **d**) The data for all four cells was qualitatively similar. The adaptation index was quite similar in control medium and in 2 μM strychnine. For one cell, the adaptation index was not significant for the low-contrast epochs; this point is not plotted.

tation at several levels along the bipolar pathway (K.J. Kim and F. Rieke, *IOVS* **41**, S937, 2000). Assuming that similar mechanisms are present in bipolar cells of mammals, they could account for the local adaptation observed here.

From previous work, we know that there are multiple sites of retinal adaptation to luminance (stimulus intensity). These range in location from the photoreceptor level to the inner plexiform layer, and have time courses that range from milliseconds to seconds to minutes[1]. The spatial extent of the neural elements' sampling luminance also varies widely, ranging from the tiny photoreceptor[32] to the wide-field dopaminergic amacrine cell[33]. They include an intermediate-sized element[34], roughly comparable in size to the local element revealed in our experiments. (The two mechanisms are unlikely to be identical because our stimuli should not cause luminance adaptation.) These varied mechanisms work in concert to maintain the retina's sensitivity to small changes in stimulus intensity despite the eight log-unit variation in absolute luminance experienced in the natural environment.

Analogously, multiple mechanisms of adaptation to contrast seem to exist in the retina. Classic experiments[1–5,7] describe a form of contrast gain control that samples contrast over a large region (millimeters) and rapidly shifts (~100 ms) the contrast–response function of retinal ganglion cells. The present results describe a much slower adaptation for various large-field stimuli than for small ones. (When similar experiments used full-field illumination, the adaptation was slower still[8].) Thus, even within the contrast adaptation protocol, different experimental conditions reveal different facets of the retina's regulation of its input–output relationships.

Most previous models postulate that the retina contains a single contrast gain-control mechanism, but faster rates of adaptation for small stimuli than for larger ones, strikingly apparent in our experiments (**Fig. 4**), are hard to explain with a single mechanism. As noted above, our results point to the bipolar cell pathway as one site of contrast adaptation. However, if a single mechanism confined to the bipolar cell were the only one, there would be no reason for the rate of adaptation to be slower for larger stimuli than for smaller ones. This paradoxical finding would seem to require some second mechanism that causes a slower rate of adaptation for large stimuli. As in the case of luminance adaptation, a retina that contains more than 50 types of neurons may use multiple forms of contrast adaptation, tuned to different aspects of the visual scene.

Local contrast adaptation would have functional consequences different from those of the broader types that have been described. Adaptation on a wide spatial scale would be useful for adjusting to the large spatial averages of the visual scene, for example, when a clear day turns into a hazy one. In contrast, the local adaptation that we describe here would function to desensitize the retina to small regions of high-contrast, whose location would vary as with head and eye movements. A quicker adaptation to small stimuli than to large could be designed to match the probabilities of change in the natural world. In the natural world, large objects change more slowly than small ones. Teleologically, it would seem sensible for

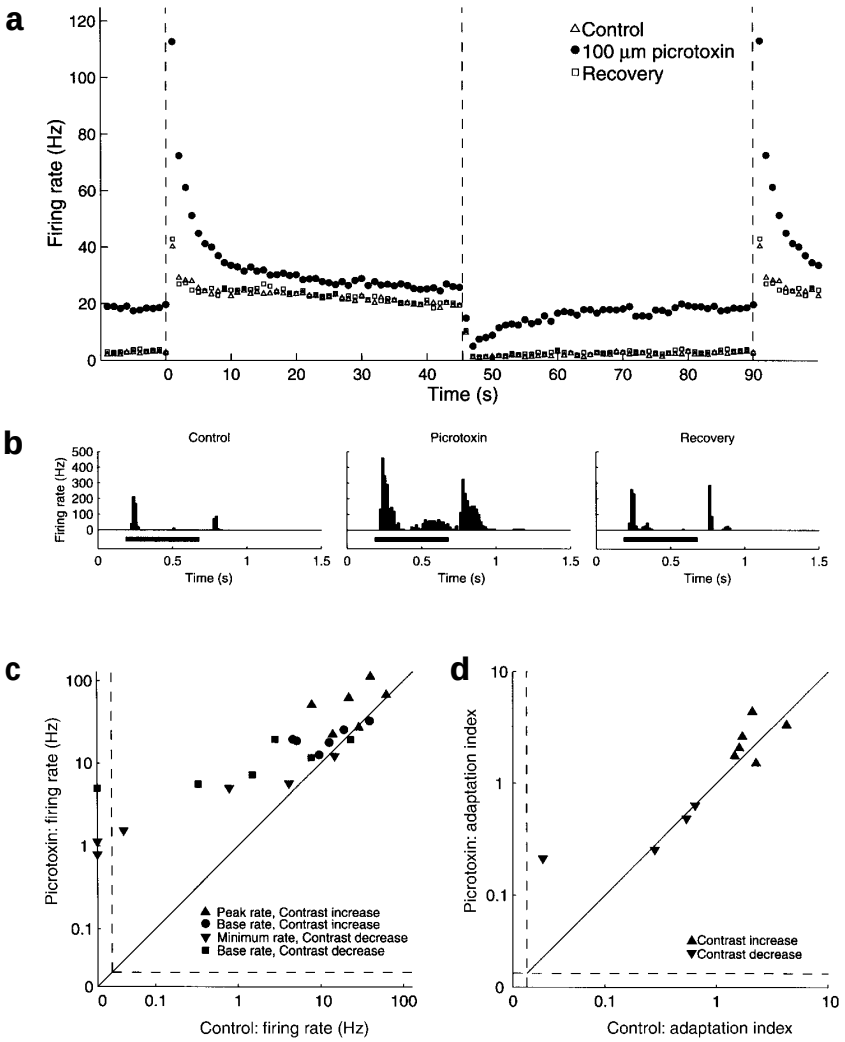

Fig. 7. Contrast adaptation in the presence of picrotoxin, an antagonist of $GABA_A$ and $GABA_C$ receptors. (**a**) Although the visual response of this ON direction-selective ganglion cell was significantly increased and prolonged in the presence of 100 μM picrotoxin, the phenomenon of contrast adaptation was nonetheless preserved. (**b**) The response of the cell shown in (**a**) to the onset and offset of a 500-μm spot of light (black bar, light ON, 500 ms). In the presence of 100 μM picrotoxin (middle), the cell's response was greatly enhanced and prolonged as compared to the control (left) and recovery conditions (right). These changes in the response to a simple spot of light provide a positive control for the drug. (**c**) In the presence of picrotoxin (50 μM, $n = 2$; 100 μM, $n = 4$), the cells' visual response was either unchanged or increased as in (**a**). Both 50 μM and 100 μM picrotoxin produced qualitatively similar responses. (**d**) The adaptation indices following step changes in contrast did not qualitatively change in the presence of an antagonist of $GABA_A$ and $GABA_C$ receptors relative to control. For two cells, the adaptation index was not significant for the low-contrast epoch under control conditions; these two points are not plotted.

the system to adapt slowly to the global averages of the visual image, which in the extreme, vary only when the animal moves from one environment to another, and quickly to more specific features.

Methods

Preparation and maintenance of *in vitro* retinas. All protocols were approved by the Subcommittee on Research Animal Care of the Massachusetts General Hospital. Extracellular recordings were done from isolated rabbit retina as previously described[23,35–37]. The retina was isolated in Ames medium (Sigma, St. Louis, Missouri) bubbled with O_2/CO_2 (95%:5%). A piece of retina, 5–12 mm on a side, was affixed to a glass coverslip[36], placed inside the recording chamber mounted on a fluorescence microscope (Axioskop FS, Zeiss, Thornwood, New York) and superfused with oxygenated Ames medium at 35–37°C.

Electrophysiology. Of the 47 cells examined in this study, we recorded from 40 using tungsten electrodes (tungsten-in-glass[38] or catalog number 25-08-2, FHC, Brunswick, Maine). The remaining seven cells were recorded using a loose-seal cell-attached patch-clamp technique[23,27]. Signals were amplified, filtered and digitized as previously described[37]. In all cases, action potentials were discriminated *post hoc*, before further analyses.

Pharmacology. We used the upper range of the concentrations generally used to block GABA and glycine receptors: 2 μM strychnine (Research Biochemicals, Natick, Massachusetts) and 50–100 μM picrotoxin (Sigma)[21,36,39,40]. When the source of the perfusate was switched from the control Ames medium to the test solution, the solution in the recording chamber was exchanged within minutes. The new solution was perfused for 30–45 minutes before experimental data were acquired.

Visual stimuli. Visual stimuli were created on a computer monitor (Nokia, Sausalito, California) and reflected, via a substage mirror, through a 20× objective (LD Achroplan; NA, 0.4; Zeiss) or a 5× objective (Plan-Neofluar; NA, 0.15; Zeiss), which replaced the microscope's condenser. Once the tissue had been placed in the perfusion chamber, the image of the monitor was focused by projecting a test square onto the preparation and adjusting the substage objective until the square was sharply in focus. The stimulus was a flickering checkerboard composed of 15×15 squares whose luminances were independently modulated every 14.2 ms or occasionally every 28.4 ms. The background was set to mean luminance. In some experiments, a subset of these 225 pixels was used while the remainder were fixed at mean luminance. The width of the squares in the checkerboard ranged from 104 to 460 μm (approximately 0.6 to 2.7 degrees of visual angle). The monitor was calibrated with an LS-100 luminance meter (Minolta, Ramsey, New Jersey) and its nonlinear input–output relationship was corrected with a software look-up table. The mean luminance of the monitor was between 1 and 10 cd/m^2. A photodiode (Hammamatsu, Middlesex, New Jersey) mounted on the microscope stage was used to calibrate the stimulus luminance at the position of the preparation and to confirm that transient changes in the intensity of the monitor during stimulus transitions did not occur. Stimuli falling on the retina were primarily in the mesopic range.

During a typical experiment, the contrast of the stimulus alternated from 100% to 20–50% every 45 s for a total of 25 high-contrast/low-contrast pairs, unless otherwise noted. The mean luminances of the stimuli were always constant. Each contrast pair was generated using a different binary pseudorandom sequence[41,42]. The first contrast pair of every experiment was discarded because it included a transition from mean luminance. Error bars in the figures represent standard errors of the mean firing rates and are almost always smaller than the symbols.

We defined the peak or minimum firing rates as those achieved in the first or second time bin following the contrast change. The baseline rate was defined as the firing rate in the last time bin of the contrast epoch. The 'adaptation index' was the ratio between these two numbers[10]. The 'decay' and 'recovery' indices denote the time bin for which the response had decayed or recovered by 66% following the contrast change. If the two firing rates did not have a difference of at least 1 Hz (~±4 standard errors) when the average response was binned at 1 s, we set the adaptation index to 1; the decay and recovery indices were therefore undefined. We then calculated the adaptation, decay and recovery indices for the bin width noted in the text. In the summary figures (**Figs. 3**, **5**, **6** and **7**), we used the adaptation index as a measure of the polarity of the adaptation. An adaptation index greater than 1 reflected a decay in firing rate, whereas an adaptation index less than 1 reflected an increase in firing rate during the epoch.

In separate experiments, the neuron's spatiotemporal receptive field was determined by calculating the spike-triggered stimulus average for the cell[43]. In the receptive fields shown in Fig. 4, red indicates where the cell was excited by dark pixels of the stimulus or inhibited by light pixels; green indicates where the cell was excited by light pixels or inhibited by dark pixels (that is, red, OFF; green, ON). The cells were also characterized using several other techniques. For example, the cells' responses to moving gratings (eight directions) were used to identify direction-selective cells. These data, coupled with the shape of the autocorrelogram[44] and the morphological features of the cells (see below), were used to classify the recorded ganglion cells[35,44–50]. After the recording session, the ganglion cell was injected with 4% Lucifer Yellow as previously described[35,36].

Acknowledgements

We thank R. Rockhill for technical assistance. S.P.B. was supported by a Howard Hughes Medical Institute Predoctoral Fellowship. R.H.M. is a Senior Investigator of Research to Prevent Blindness.

Received 19 July; Accepted 27 October 2000

1. Shapley, R. & Enroth-Cugell, C. Visual adaptation and retinal gain controls. *Prog. Ret. Res.* **3**, 263–346 (1984).
2. Shapley, R. & Victor, J. D. The effect of contrast on the transfer properties of cat retinal ganglion cells. *J. Physiol. Lond.* **285**, 275–298 (1978).
3. Shapley, R. M. & Victor, J. D. Nonlinear spatial summation and the contrast gain control of cat retinal ganglion cells. *J. Physiol. Lond.* **290**, 141–161 (1979).
4. Shapley, R. M. & Victor, J. D. The effect of contrast on the non-linear response of the Y cell. *J. Physiol. Lond.* **302**, 535–547 (1980).
5. Shapley, R. M. & Victor, J. D. How the contrast gain control modifies the frequency responses of cat retinal ganglion cells. *J. Physiol. Lond.* **318**, 161–179 (1981).
6. Benardete, E. A., Kaplan, E. & Knight, B. W. Contrast gain control in the primate retina: P cells are not X-like, some M cells are. *Vis. Neurosci.* **8**, 483–486 (1992).
7. Enroth-Cugell, C. & Jakiela, H. G. Suppression of cat retinal ganglion cell responses by moving patterns. *J. Physiol. Lond.* **302**, 49–72 (1980).
8. Smirnakis, S. M., Berry, M. J., Warland, D. K., Bialek, W. & Meister, M. Adaptation of retinal processing to image contrast and spatial scale. *Nature* **386**, 69–73 (1997).
9. Shapley, R. Retinal physiology: adapting to the changing scene. *Curr. Biol.* **7**, R421–423 (1997).
10. Albrecht, D. G., Farrar, S. B. & Hamilton, D. B. Spatial contrast adaptation characteristics of neurones recorded in the cat's visual cortex. *J. Physiol. Lond.* **347**, 713–739 (1984).
11. Ohzawa, I., Sclar, G. & Freeman, R. D. Contrast gain control in the cat's visual system. *J. Neurophysiol.* **54**, 651–667 (1985).
12. Sanchez-Vives, M. V., Nowak, L. G. & McCormick, D. A. Membrane mechanisms underlying contrast adaptation in cat area 17 *in vivo*. *J. Neurosci.* **20**, 4267–4285 (2000).
13. Maddess, T., McCourt, M. E., Blakeslee, B. & Cunningham, R. B. Factors governing the adaptation of cells in area-17 of the cat visual cortex. *Biol. Cybern.* **59**, 229–236 (1988).
14. Vaney, D. I. The mosaic of amacrine cells in the mammalian retina. *Prog. Ret. Res.* **9**, 49–100 (1991).
15. MacNeil, M. A. & Masland, R. H. Extreme diversity among amacrine cells: implications for function. *Neuron* **20**, 971–982 (1998).
16. MacNeil, M. A., Heussy, J. K., Dacheux, R. F., Raviola, E. & Masland, R. H. The shapes and numbers of amacrine cells: matching of photofilled with Golgi-stained cells in the rabbit retina and comparison with other mammalian species. *J. Comp. Neurol.* **413**, 305–326 (1999).
17. Koontz, M. A., Hendrickson, L. E., Brace, S. T. & Hendrickson, A. E. Immunocytochemical localization of GABA and glycine in amacrine and displaced amacrine cells of macaque monkey retina. *Vision Res.* **33**, 2617–2628 (1993).
18. Kalloniatis, M., Marc, R. E. & Murry, R. F. Amino acid signatures in the primate retina. *J. Neurosci.* **16**, 6807–6829 (1996).
19. Crook, D. K. & Pow, D. V. Analysis of the distribution of glycine and GABA in amacrine cells of the developing rabbit retina: a comparison with the ontogeny of a functional GABA transport system in retinal neurons. *Vis. Neurosci.* **14**, 751–763 (1997).
20. Ehinger, B., Ottersen, O. P., Storm-Mathisen, J. & Dowling, J. E. Bipolar cells in the turtle retina are strongly immunoreactive for glutamate. *Proc. Natl. Acad. Sci. USA* **85**, 8321–8325 (1988).
21. Lukasiewicz, P. D. & Wong, R. O. L. $GABA_C$ receptors on ferret retinal bipolar cells: A diversity of subtypes in mammals? *Vis. Neurosci.* **14**, 989–994 (1997).
22. Mills, S. L. & Massey, S. C. Distribution and coverage of A- and B-type horizontal cells stained with Neurobiotin in the rabbit retina. *Vis. Neurosci.* **11**, 549–560 (1994).
23. Peters, B. N. & Masland, R. H. Responses to light of starburst amacrine cells. *J. Neurophysiol.* **75**, 469–480 (1996).
24. Taylor, W. R. & Wässle, H. Receptive field properties of starburst cholinergic amacrine cells in the rabbit retina. *Eur. J. Neurosci.* **7**, 2308–2321 (1995).
25. Stafford, D. K. & Dacey, D. M. Physiology of the A1 amacrine: a spiking, axon-bearing interneuron of the macaque monkey retina. *Vis. Neurosci.* **14**, 507–522 (1997).
26. Taylor, W. R. Response properties of long-range axon-bearing amacrine cells in the dark-adapted rabbit retina. *Vis. Neurosci.* **13**, 599–604 (1996).
27. Taylor, W. R. TTX attenuates surround inhibition in rabbit retinal ganglion cells. *Vis. Neurosci.* **16**, 285–290 (1999).
28. Mills, S. L. & Massey, S. C. Morphology of bipolar cells labeled by DAPI in the rabbit retina. *J. Comp. Neurol.* **321**, 133–149 (1992).
29. Massey, S. C. & Mills, S. L. A calbindin-immunoreactive cone bipolar cell type in the rabbit retina. *J. Comp. Neurol.* **366**, 15–33 (1996).
30. Brown, S. P. & Masland, R. H. Costratification of a population of bipolar cells with the direction-selective circuitry of the rabbit retina. *J. Comp. Neurol.* **408**, 97–106 (1999).
31. Sterling, P. in *The Synaptic Organization of the Brain* (ed. Shepherd, G.) 205–253 (Oxford Univ. Press, Oxford, 1998).
32. Perlman, I. & Normann, R. A. Light adaptation and sensitivity controlling mechanisms in vertebrate photoreceptors. *Prog. Ret. Eye Res.* **17**, 523–563 (1998).
33. Witkovsky, P. & Dearry, A. Functional roles of dopamine in the vertebrate retina. *Prog. Ret. Res.* **11**, 247–292 (1991).
34. Cleland, B. G. & Freeman, A. W. Visual adaptation is highly localized in the cat's retina. *J. Physiol. Lond.* **404**, 591–611 (1988).
35. Yang, G. & Masland, R. H. Receptive fields and dendritic structure of directionally selective retinal ganglion cells. *J. Neurosci.* **14**, 5267–5280 (1994).
36. He, S. & Masland, R. H. Retinal direction selectivity after targeted laser ablation of starburst amacrine cells. *Nature* **389**, 378–382 (1997).
37. Brown, S. P., He, S. & Masland, R. H. Receptive field microstructure and dendritic geometry of retinal ganglion cells. *Neuron* **27**, 371–383 (2000).
38. Levick, W. R. Another tungsten microelectrode. *Med. Biol. Eng.* **10**, 510–515 (1972).
39. Zhou, Z. J. & Fain, G. L. Neurotransmitter receptors of starburst amacrine cells in rabbit retinal slices. *J. Neurosci.* **15**, 5334–5345 (1995).
40. Massey, S. C., Linn, D. M., Kittila, C. A. & Mirza, W. Contributions of $GABA_A$ receptors and $GABA_C$ receptors to acetylcholine release and directional selectivity in the rabbit retina. *Vis. Neurosci.* **14**, 939–948 (1997).
41. Park, S. K. & Miller, K. W. Random number generators: good ones are hard to find. *Communications ACM* **31**, 1192–1201 (1988).
42. Reid, R. C., Victor, J. D. & Shapley, R. M. The use of m-sequences in the analysis of visual neurons: linear receptive field properties. *Vis. Neurosci.* **14**, 1015–1027 (1997).
43. De Boer, E. & Kuyper, P. Trigger correlation. *IEEE Trans. Biomed. Eng.* **15**, 169–179 (1968).
44. DeVries, S. H. & Baylor, D. A. Mosaic arrangement of ganglion cell receptive fields in rabbit retina. *J. Neurophysiol.* **78**, 2048–2060 (1997).
45. Levick, W. R. Receptive fields and trigger features of ganglion cells in the visual streak of the rabbit's retina. *J. Physiol. Lond.* **188**, 285–307 (1967).
46. Buhl, E. H. & Peichl, L. Morphology of rabbit retinal ganglion cells projecting to the medial terminal nucleus of the accessory optic system. *J. Comp. Neurol.* **253**, 163–174 (1986).
47. Peichl, L., Buhl, E. H. & Boycott, B. B. Alpha ganglion cells in the rabbit retina. *J. Comp. Neurol.* **263**, 25–41 (1987).
48. Amthor, F. R., Takahashi, E. S. & Oyster, C. W. Morphologies of rabbit retinal ganglion cells with complex receptive fields. *J. Comp. Neurol.* **280**, 97–121 (1989).
49. Amthor, F. R., Takahashi, E. S. & Oyster, C. W. Morphologies of rabbit retinal ganglion cells with concentric receptive fields. *J. Comp. Neurol.* **280**, 72–96 (1989).
50. He, S. & Masland, R. H. ON direction-selective ganglion cells in the rabbit retina: dendritic morphology and pattern of fasciculation. *Vis. Neurosci.* **15**, 369–375 (1998).